catalysts

MDPI

Article

Synthesis of HZSM-5 Rich in Paired Al and Its Catalytic Performance for Propane Aromatization

Dezhi Shi [1,2,†], Sen Wang [1,2,†], Hao Wang [1,*], Pengfei Wang [1], Li Zhang [1,2], Zhangfeng Qin [1], Jianguo Wang [1], Huaqing Zhu [1,*] and Weibin Fan [1,*]

[1] State Key Laboratory of Coal Conversion, Institute of Coal Chemistry, Chinese Academy of Sciences, 27 South Taoyuan Road, Taiyuan, Shanxi 030001, China; shidezhi@sxicc.ac.cn (D.S.); wangsen@sxicc.ac.cn (S.W.); wangpf@sxicc.ac.cn (P.W.); zhangli603@sxicc.ac.cn (L.Z.); qzhf@sxicc.ac.cn (Z.Q.); jgwang@sxicc.ac.cn (J.W.)

[2] University of Chinese Academy of Sciences, Beijing 100049, China

* Correspondence: wanghao@sxicc.ac.cn (H.W.); zhuhq@sxicc.ac.cn (H.Z.); fanwb@sxicc.ac.cn (W.F.)

† These authors equally contributed to this work.

Received: 26 May 2020; Accepted: 2 June 2020; Published: 3 June 2020

Abstract: A series of HZSM-5 catalysts with similar Si/Al_F mole ratio, textual properties and morphology, but different contents of Al_F pairs, were synthesized by controlling the Na/Al molar ratios in the precursor gel and used for propane aromatization. It is shown that the catalyst with a Na/Al molar ratio of 0.8 in the synthetic gel possesses the highest paired Al_F concentration (64.4%) and shows higher propane conversion (38.2%) and aromatics selectivity (19.7 wt.%). Propane pulse experiments, micro reactor activity estimation, Operando diffuse reflectance ultraviolet-visible (DR UV-vis) spectroscopy and Fourier Transform Infrared Spectroscopy (FTIR) analysis of coke species deposited on the catalysts provide evidence that Al_F pairs in the ZSM-5 framework promote oligomerization and cyclization reactions of olefins, and then produce more aromatics. Density Functional Theory (DFT) calculations demonstrate that the cyclization of olefins and hydride transfer reaction occurring on Al_F pairs in HZSM-5 zeolite show a lower free energy barrier and a higher rate constant than those on single Al_F, indicating that the structure of Al_F pairs in the HZSM-5 zeolite has a stronger electrostatic stabilization effect on the transition states than that of single Al_F.

Keywords: HZSM-5; Al pairs; propane aromatization; Operando DR UV-vis; DFT calculations

1. Introduction

The aromatization of light alkanes (mainly propane and butane) has been extensively studied for almost three decades due to its importance in the economic and strategic fields [1,2]. For the propane aromatization process, Zn, Pt and Ga-promoted ZSM-5 catalysts are recognized as effective bifunctional catalysts [3–15]. Light alkane chain growth on bifunctional catalysts involves dehydrogenation, oligomerization, cyclization, and aromatization steps, which proceed in parallel with acid-catalyzed and thermal cracking reactions. In general, metal (Zn, Pt and Ga) species are responsible for dehydrogenation processes, while zeolitic acid sites serve catalytic functions for the oligomerization and cyclization steps [3,12,13]. ZSM-5 zeolite has been proved to be the most promising component of aromatization catalysts because of its high hydrothermal stability, unique shape-selective behavior, adjustable acidity and suitable crystal structure [1,3]. However, few studies have examined the influence of the framework aluminum (Al_F) distribution of HZSM-5 zeolites on its propane aromatization catalytic performance.

In the framework of HZSM-5, there are two types of Al species, i.e., paired Al and single Al. The term paired Al refers to the Al–O–(Si–O)$_{1,2}$–Al sequences, whereas isolated single Al atoms represent Al–O–(Si–O)$_{\geq 3}$–Al sequences [16]. The content of Al$_F$ pairs and single Al$_F$ can be estimated by using exchanged Co(II)-ZSM-5 samples. Hexaaquocomplexes of Co^{2+} ions can balance the negative charges generated by two close Al atoms, named as Al$_F$ pairs (located in one framework ring or different framework rings), whereas the single Al atom is defined as one Al atom sitting in a five- or six-membered ring that cannot be coordinated by Co^{2+} ions [17,18]. Al$_F$ distribution can be regulated in the synthesis process of the ZSM-5 zeolites by changing the Si source (such as TEOS, colloidal silica and sodium silicate), Al source ($AlCl_3$, $Al(NO_3)_3$, $NaAlO_2$ and $Al(OH)_3$), sodium content, and organic templating [17,19–21]. Biligetu et al. [19] reported that ZSM-5 zeolites with different framework Al achieved by adding various alcohols exhibit different methanol-to-olefins (MTO) performance, whereby a relatively large number of Al$_F$ pairs in the catalyst produces more ethene by enhancing the ''aromatics-based cycle" [22]. Sazama and co-workers [20] found that Al$_F$ pairs in HZSM-5 framework were beneficial to 1-butene oligomerization in 1-butene conversion, whereas single Al$_F$ was favorable to 1-butene cracking and gave higher selectivity to lower olefins. Song et al. [23] reported that Al$_F$ pairs cooperatively catalyze alkane cracking at higher turnover rates than on single Al$_F$ and the apparent activation entropies become less negative at higher Al$_F$ pair concentrations although the apparent activation energies are similar on HZSM-5 catalysts with different concentrations of single Al$_F$ and Al$_F$ pairs on different alkane reactants (propane, *n*-butane, and *n*-pentane); thus, enhanced cracking rates at these Al$_F$ pairs are mainly due to more positive intrinsic activation entropies. Tabor et al. reported that turnover rates for the conversion of propene to C_4-C_9 olefins and to BTX aromatics are 5–8 times and 20 times higher, respectively, over Al$_F$ pairs than those over single Al$_F$ [24]. It is thus firmly believed that the distribution of Al$_F$ in HZSM-5 must be an important factor in catalytic activity and therefore, it is necessary to investigate the impact of Al$_F$ distribution in HZSM-5 on propane aromatization.

In this work, a series of HZSM-5 catalysts with different contents of Al$_F$ pairs were synthesized by controlling the Na/Al molar ratios in the precursor gels and HZSM-5 catalysts with similar Si/Al$_F$ molar ratio, textual properties, and morphology were applied to propane aromatization reaction. It is found that the Al$_F$ pair content in HZSM-5 has a significant influence on propane conversion and selectivity to aromatics. Operando UV-vis spectroscopy and gas chromatography-mass spectrometry (GC-MS) and theoretical calculations revealed that Al$_F$ pairs in HZSM-5 framework promote oligomerization and cyclization reactions of olefins in propane aromatization. The structure of Al$_F$ pairs in the ZSM-5 zeolite shows stronger electrostatic stabilization effect on the transition states than that of single Al$_F$. These results gave new insights into the impact of Al$_F$ distribution in HZSM-5 on propane aromatization, which should facilitate the design of high performance catalysts.

2. Results and Discussion

2.1. Physicochemical Properties of Catalysts

The X-ray diffraction patterns of the catalysts are shown in Figure 1. All of the catalysts exhibit the typical reflections of a MFI zeolite-type framework with similar crystallinity. The lattice parameters of the catalysts calculated trough Rietveld refinement of the XRD data are shown in Table 1. All of the catalysts have similar cell parameters. The SEM images of the catalysts are shown in Figure 2. All of the catalysts exhibit similar morphology and small uniform particles with an average size of ~100 nm. The subtle difference in these four samples is that pictures of samples HZ(0), HZ(0.4) and HZ(0.8) shows almost the same particle agglomerations while sample HZ(1.1) shows smaller particle agglomerations.

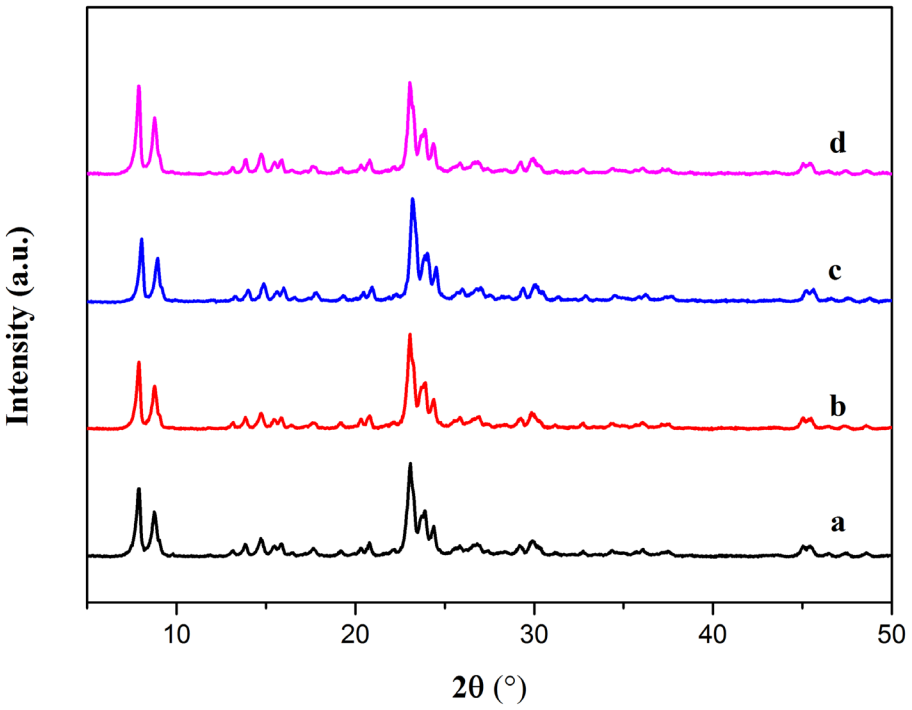

Figure 1. XRD patterns of HZSM-5 catalysts with different Na/Al ratios in synthesis gels. (**a**) HZ(0), (**b**) HZ(0.4), (**c**) HZ(0.8), and (**d**) HZ(1.1).

Table 1. Crystallite and lattice parameters of catalysts.

Catalyst	Crystal System	Lattice Parameters					
		a (Å)	b (Å)	c (Å)	α	β	γ
HZ(0)	Orthorhombic	20.091	19.899	13.384	90°	90°	90°
HZ(0.4)	Orthorhombic	20.102	19.902	13.389	90°	90°	90°
HZ(0.8)	Orthorhombic	20.090	19.905	13.389	90°	90°	90°
HZ(1.1)	Orthorhombic	20.098	19.907	13.390	90°	90°	90°

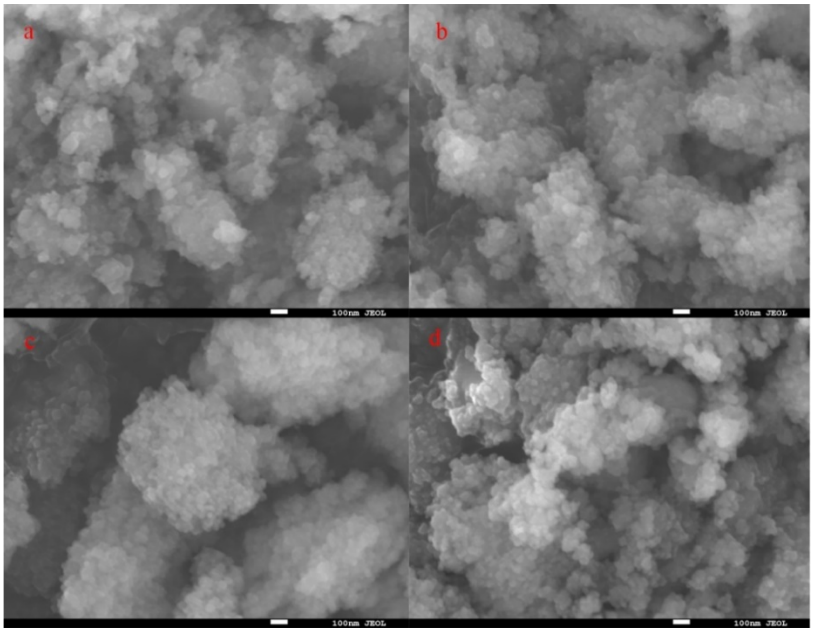

Figure 2. SEM images of the HZSM-5 catalysts with different Na/Al ratios in synthesis gels. (**a**) HZ(0), (**b**) HZ(0.4), (**c**) HZ(0.8), and (**d**) HZ(1.1).

The textual properties and chemical composition of the catalysts are summarized in Table 2. The catalysts have similar surface areas, pore volumes, pore size distributions and Si/Al ratios.

Table 2. Elemental composition, textual properties and Al distribution of HZSM catalysts with different Na/Al ratios in synthesis gels.

Catalysts	Si/Al [a]	Si/Al_F [b]	Al_F/Al_{total} [b] (%)	S_{total} [c] (m^2g^{-1})	S_{micro} [d] (m^2g^{-1})	V_{total} [e] (m^3g^{-1})	V_{micro} [d] (m^3g^{-1})	PSD [f] (nm)
HZ(0)	42	43	97.2	420	256	0.45	0.11	0.772~0.879
HZ(0.4)	37	38	97.9	380	257	0.34	0.11	0.772~0.879
HZ(0.8)	38	40	95.7	363	267	0.28	0.12	0.772~0.879
HZ(1.1)	38	39	97.6	383	260	0.33	0.11	0.772~0.879

[a] Measured by ICP-OES. [b] Determined by ^{27}Al MAS NMR. [c] Total specific surface area determined by BET equation. [d] Micropore surface area and micropore volume determined by t-plot method. [e] Total pore volume determined by volume adsorbed at $p/p^0 = 0.99$. [f] Pore size distribution (PSD) was acquired by Density Functional Theory (DFT) method.

The ^{27}Al-MAS NMR spectra of the catalysts are shown in Figure 3. All samples exhibit an intense peak at about 55 ppm, ascribed to tetrahedral framework Al and a weaker peak at approximately 0 ppm attributed to octahedral extra-framework Al. It is noticed that the overwhelming majority of Al species is framework Al. The Si/Al_F ratios of the catalysts acquired from ^{27}Al-MAS NMR analysis closely match their Si/Al ratios obtained by ICP-OES, indicating that almost all of Al atoms are present as Al_F in the ZSM-5 framework.

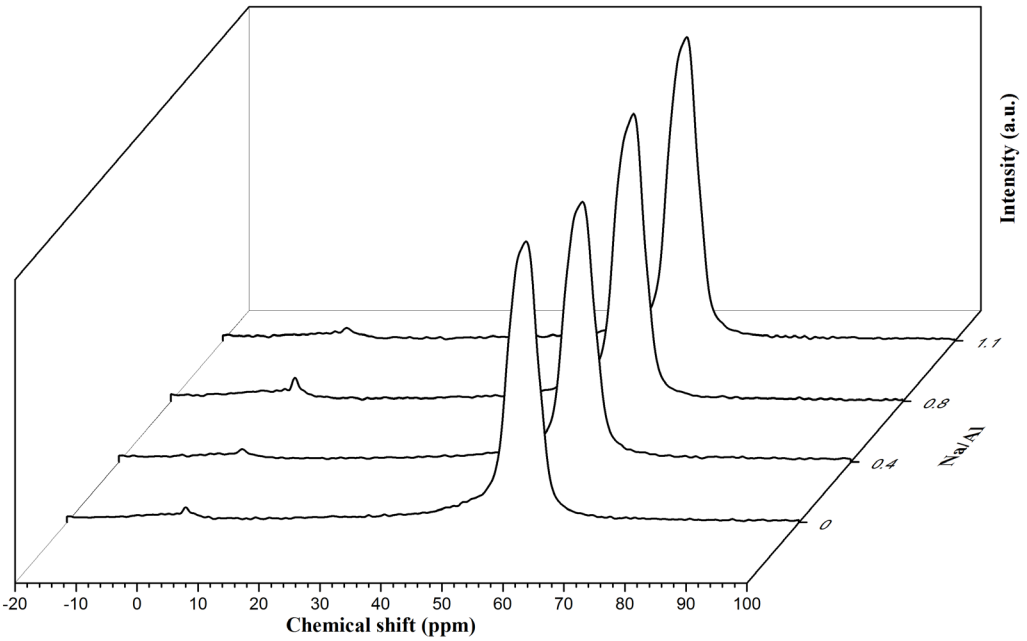

Figure 3. ^{27}Al-MAS NMR spectra of HZ(0), HZ(0.4), HZ(0.8) and HZ(1.1) catalysts.

Pyridine-adsorption infrared spectroscopy and NH_3-TPD were employed to characterize the acidic properties of the catalysts, and the results are shown in Table 3. The catalysts possess similar numbers of Brönsted and Lewis/weak and strong acid sites, which is in good agreement of the Si/Al_F ratios. On the whole, the as-prepared catalysts exhibit similar morphology, textual properties, Si/Al_F ratio and acidic property.

Table 3. Acidic properties of the catalysts based on pyridine adsorption IR and NH_3-TPD analysis.

Catalysts	Acidity by Py-IR (mmol g^{-1}) [a]			Acidity by NH_3-TPD (mmol g^{-1}) [b]		
	Brønsted	Lewis	Total	Strong	Weak	Total
HZ(0)	0.20	0.04	0.24	0.32	0.28	0.62
HZ(0.4)	0.22	0.04	0.26	0.37	0.27	0.64
HZ(0.8)	0.22	0.05	0.27	0.36	0.27	0.63
HZ(1.1)	0.21	0.03	0.24	0.36	0.28	0.64

[a] The quantities of Brönsted and Lewis acid sites were calculated from the Py-IR spectra. [b] The quantities of weak and strong acid sites determined by NH_3-TPD were measured by the amounts of ammonia desorbed at 120–250 and 250–500 °C, respectively.

2.2. Al distribution in the ZSM-5 Framework

The proportions of framework Al species (Al_F pairs and single Al_F) in the different Co(II)-ZSM-5 samples are listed in Table 4. It is found that the fraction of Al_F pairs in as-prepared catalysts increases from 54.2% to 64.4% with the increase of the Na/Al molar ratio in the precursor gels from 0 to 0.8, and then decreases with further increase of the Na/Al ratio.

Table 4. Al distribution of Co-type ZSM-5 and HZSM-5.

Samples	Al_F Content (%)			Al Pair Distribution (%)[c]			Al Content by NMR (%)	
	Al_{single} [a]	Al_{pairs} [a]	(2Co + Na)/Al [b]	α	β	γ	$Al_{(54)}$ [d]	$Al_{(56)}$ [d]
Co/ZSM-5(0)	45.8	54.2	0.99	14	64	22	31	29
Co/ZSM-5(0.4)	42.1	57.9	0.99	10	66	24	33	27
Co/ZSM-5(0.8)	35.6	64.4	0.96	10	65	25	33	27
Co/ZSM-5(1.1)	40.4	59.6	0.97	7	68	25	31	27

[a] The contents of single Al and Al pairs (2Co/Al) were calculated by the equations $[Al_{single}] = [Al_{total}]-2[Co_{max}]$ and $[Al_{pairs}] = 2[Co_{max}]$, where Al_{total} and Co_{max} were determined by ICP-OES. [b] The (2Co + Na)/Al ratio was determined by ICP-OES. [c] The distribution of different Al pairs types (α, β, and γ) was determined by the deconvolution of Co(II) UV-vis-DR spectroscopy of Co-type ZSM-5 zeolites. [d] The contents of $Al_{(54)}$ and $Al_{(56)}$ peaks were determined by deconvolution of the ^{27}Al MAS NMR spectra of H-ZSM-5 catalysts.

Co(II) UV-vis-DRS was employed to investigate the distribution of Al_F pairs in Co/ZSM-5 zeolites. The spectra were deconvoluted into seven bands of three Co(II) cations types coordinated with different Al_F pairs T-sites. The relative concentrations of α-type Co(II) ions in the straight channel, β-type Co(II) ions in the channel intersections and γ-type Co(II) ions in the sinusoidal channels are also given in Table 4. Most of Al_F pairs are distributed in the channel intersection T-sites (~66%), and the relative concentrations of these three types T-sites shows the similar tendence in all of the catalysts.

^{27}Al MAS-NMR spectra were also employed to investigate the distribution of framework Al in HZSM-5 by deconvolution of the broad peak ranging from 45 to 65 ppm [17,21,25], as shown in Figure 4. Among the five peaks, the peak at 54 ppm ($Al_{(54)}$) and 56 ppm ($Al_{(56)}$) are related to the framework Al sites in the channel intersections and in straight and sinusoidal channels, respectively. The deconvolution results are listed in Table 4. Obviously, all the four samples exhibit a higher fraction of $Al_{(54)}$, suggesting that more Al_F site are distributed in channel intersections. This is in agreement with the Co(II) UV-vis-DRS results.

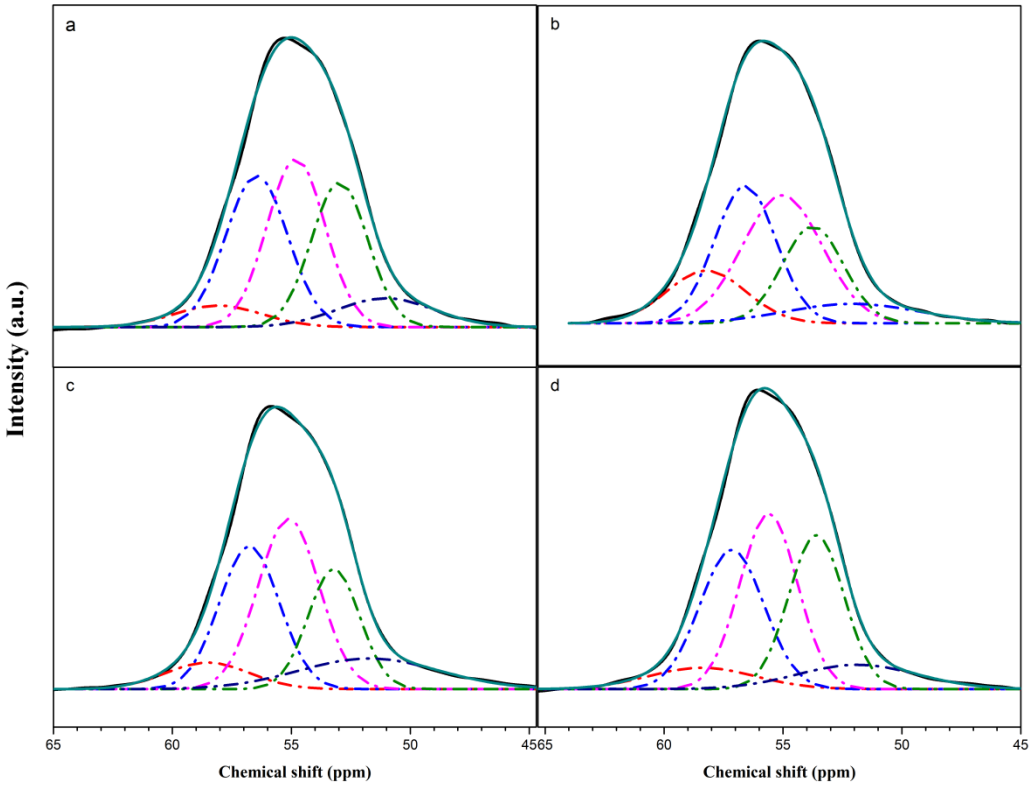

Figure 4. Deconvolution of the ^{27}Al-MAS NMR spectra of (**a**) HZ(0), (**b**) HZ(0.4), (**c**) HZ(0.8) and (**d**) HZ(1.1) catalysts.

2.3. Catalytic Performance

2.3.1. Catalytic Performance of HZSM-5 Zeolites in the Fixed-Bed Reactor

The performance of the catalysts obtained in a fixed-bed reactor for propane aromatization is illustrated in Figure 5. The propane conversion and the aromatics selectivity exhibit the same trends along with time on stream (TOS) for all catalysts. The catalyst HZ(0.8) with more Al_F pairs shows much higher propane conversion and aromatics selectivity than the other catalysts.

The selectivity of products in propane aromatization as a function of Al_F pairs content is illuminated in Figure 6. It can be seen that the aromatics selectivity and hydrogen selectivity are increased, but the selectivity to $C_3^=$-$C_4^=$ olefins is decreased with the increasing Al_F pairs content, while the selectivity to the cracking products (methane, ethane and ethene) does not differ too much. The aromatics selectivity to HZ(0.8) catalyst is 2.3 times higher than that of HZ(0) catalyst. What's more, the coke content of the used catalysts after 24 h TOS is also shown in Figure 6. It can be seen that coke content deposited in the catalysts is increased with the increasing of Al_F pairs content, which is plotted similar to the tendence of aromatics selectivity.

Since the catalysts exhibit similar morphology, textual properties, Si/Al_F ratio and Brønsted acid sites numbers, the linear correlation between the selectivity of aromatics and olefins and Al_F pairs contents reveals that the excellent catalytic performance of HZ(0.8) is probably contributed to by the higher fraction of Al_F pairs in the catalyst.

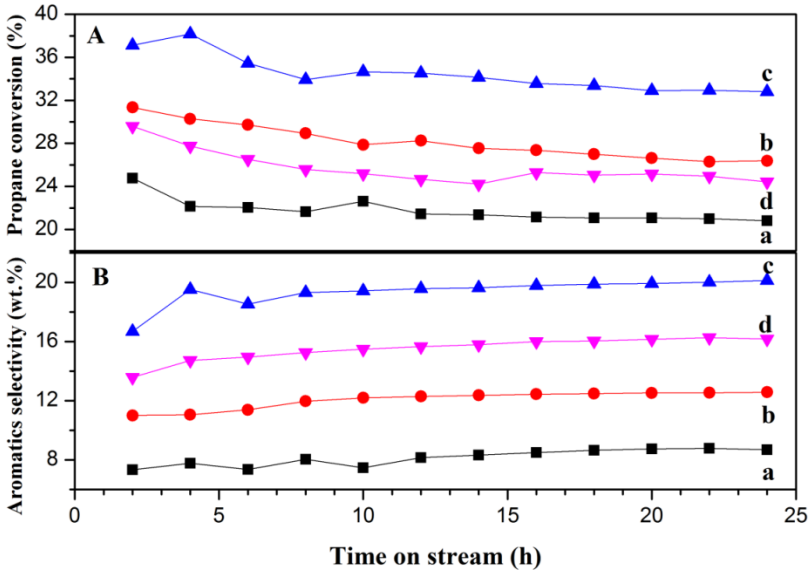

Figure 5. Propane conversion (**A**) and aromatics selectivity (**B**) with the time on stream (TOS) over HZSM-5 catalysts: HZ(0) (a), HZ(0.4) (b), HZ(0.8) (c) and HZ(1.1) (d). at 550 °C with weight hourly space velocity (WHSV) of propane being 0.6 h^{-1} and N_2/C_3H_8 ratio being 2.5 in feedstock.

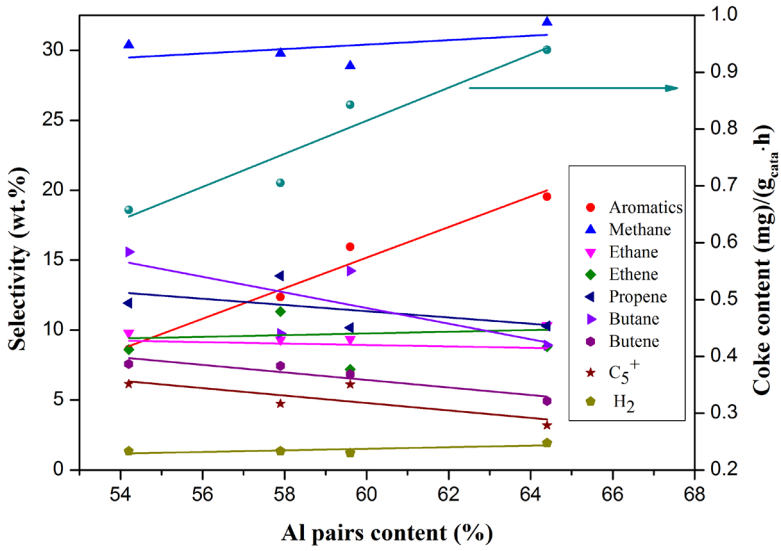

Figure 6. Product selectivity in propane aromatization at 20 h (TOS) and coke content in the used catalysts as a function of Al_F pairs content in the framework of HZSM-5 catalysts.

The reaction pathway of propane aromatization on HZSM-5 shown in Scheme 1 is well established [3]. The primary products of propane aromatization are propene and hydrogen from the dehydrogenation process, in parallel with the formation of methane and ethylene through protonic cracking reactions. Propene undergoes cyclo-oligomerization and hydrogen transfer reactions to generate aromatics and alkanes at Brønsted acid sites on HZSM-5 catalysts. In the meantime, butene and pentene obtained from cracking of C_6-C_8 alkenes may oligomerize again to form C_6-C_8 alkenes. Therefore, the trend of selectivity to aromatics increase with the increase of Al_F pair content accompanied with the decrease of olefins production may be attributed to the presence of more Al_F pairs in the catalyst, which enhances the oligomerization of alkenes and cyclization reactions to promote the formation of aromatics. The following characterization and DFT calculation will demonstrate this hypothesis particularly.

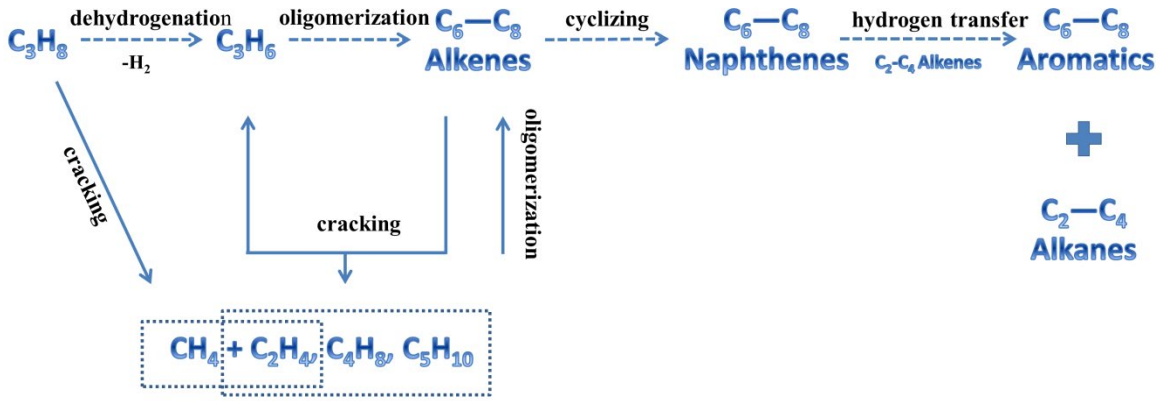

Scheme 1. Reaction pathway of propane aromatization on HZSM-5 catalysts [3].

2.3.2. Micro Reactor Activity Estimation

In order to estimate the initial products of HZ(0) and HZ(0.8) catalysts at low propane conversion, the gaseous products at a time-on-stream of 2 min on a micro reactor at 500 °C were on-line analyzed. Propane conversion are limited to 1.6% and 1.8% for HZ(0) and HZ(0.8) catalysts, respectively. The relative concentrations of gaseous products are compared in Table 5.

Table 5. Relative concentration of gaseous products for propane aromatization obtained in micro reactor experiment.

Catalysts	Aromatics Concentration (×10⁴) [a]	Olefin Concentrations [a]		
		Ethene	Propene	Butene
HZ(0)	7.71	0.924	0.159	0.015
HZ(0.8)	14.1	0.918	0.089	0.014

[a] Normalized by methane concentration in propane aromatization at 500 °C with the contact time of propane being 1.5 s.

It can be seen that the relative concentration of propene for HZ(0.8) catalyst is much lower than that of HZ(0) catalyst; on the contrary, the relative concentration of aromatics for HZ(0.8) catalyst is much higher than that of HZ(0) catalyst. Propene as the primary product of propane aromatization undergoes cyclo-oligomerization and hydrogen transfer reactions to generate aromatics and alkanes at Brønsted acid sites (single Al_F and Al_F pairs) (Figure 7). Although both single Al_F and Al_F pairs sites can catalyze propene oligomerization, experimental results demonstrate that catalyst possessing higher Al_F pairs content produces at the expense of propene and higher aromatics concentration in the products, which indicate that the presence of more Al_F pairs in the catalysts enhances the oligomerization of alkenes.

2.3.3. Pulse Experiment of Propane Aromatization

To investigate the initial products retained in the catalysts during propane aromatization, the catalytic performances of HZ(0) and HZ(0.8) catalysts were comparatively evaluated by pulse experiments at 500 °C. As illustrated in Figure 7, the products deposited on catalysts are mainly benzene, toluene, xylenes, trimethylbenzenes (triMBs) and tetramethylbenzenes (tetraMBs). Comparing with the soluble coke of two catalysts, the HZ(0.8) catalyst possesses more aromatics, especially benzene, toluene, xylenes.

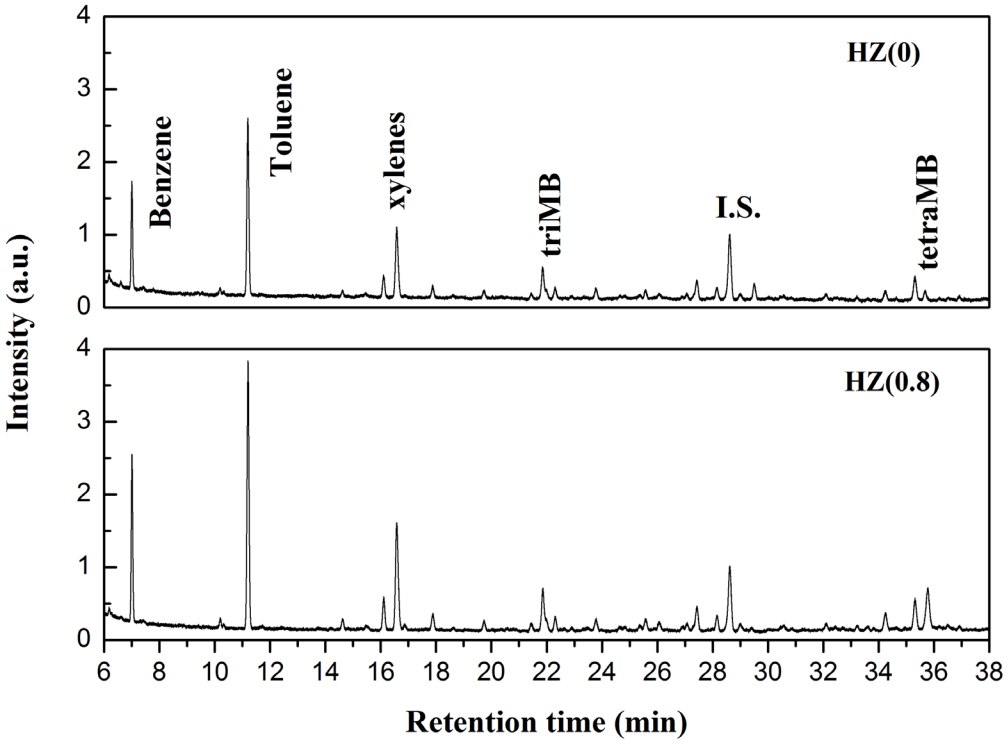

Figure 7. GC-MS spectra of the retained products in HZ(0) and HZ(0.8) catalysts after pulse of propane at 500 °C, which are normalized to the I.S. intensity.

The results of GC-MS and micro reactor activity estimation indicate more Al pairs in the catalysts enhance the oligomerization of alkenes (especially propene) and produce more aromatics, which is consistent with the results of catalytic performance tests.

2.3.4. Operando Diffuse Reflectance Ultraviolet-Visible (DR UV-vis) Spectra Experiment

It is well-known that aromatization of propane goes through dehydrogenation, oligomerization, cyclization, and aromatization steps [3,12,13,24]. Taking into account that propane dehydrogenation, as the first step of propane aromatization, can be catalyzed by metal species such as Zn, Pt and Ga etc., but the oligomerization and cyclization steps of light olefins are only catalyzed by zeolite acid sites, thus Operando diffuse reflectance ultraviolet-visible (DR UV-vis) spectra experiments were explored to investigate the formation of hydrocarbon species (mainly intermediate products) for propene conversion.

Figure 8 shows the Operando DR UV-vis spectra for conversion of propene at 250 °C over HZ(0) and HZ(0.8) catalysts, respectively. The bands located at 220~300 nm are attributed to cyclopentadienes, cyclohexadienes, neutral (methylated) benzenes, monoenyl carbocations and alkyl-substituted cyclopentenyl carbocations [26–30]. The bands centered at ca. 320~350 nm are ascribed to dienyl carbocations and low methylated benzene carbocations (such as xylenes and trimethylbenzenes) [28,31,32]. The bands at ca. 400~440 nm are assigned to highly methylated benzene carbocations (such as tetramethylbenzene, pentamethylbenzene and hexamethylbenzene) [28,30,31]. An increase in absorbance with increasing time-on-stream is observed, indicating the accumulation of the intermediate products on the zeolite catalysts during the conversion of propene. Compared with HZ(0) catalyst, more carbonaceous materials are formed on HZ(0.8) catalyst, especially those located at 250~350 nm assigned to the intermediates of aromatics originated from oligomerization and cyclization processes. The result is in good agreement with the catalytic performance tests.

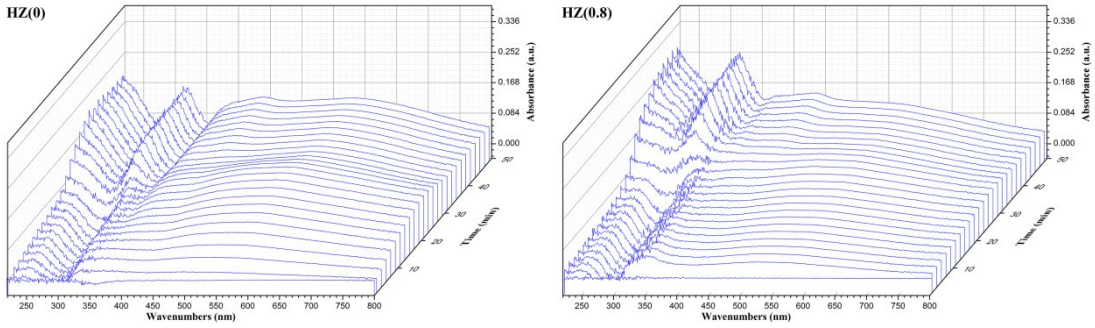

Figure 8. Operando DR UV-vis spectroscopy for conversion of propene over HZ(0) and HZ(0.8) catalysts at 250 °C.

2.4. Coke Analysis

DR UV-vis and FTIR spectra were employed to analyze the coke species deposited in the used catalysts. The DR UV-vis spectra of the used HZ(0) and HZ(0.8) catalyst are shown in Figure 9. The bands at ~330 and ~410 nm are ascribed to dienyl carbocations/low methylated benzene carbocations and highly methylated benzene carbocations, respectively [30]. As for the band at ~530 nm, it may be caused by phenanthrene, anthracene carbocations, deposited pyrene and/or more benzene rings-fused aromatic molecules [30,31]. It is noticed that the coke species are similar for these two catalysts. However, one cannot determine precise differences between the different reaction species with TOS from DR UV-vis spectra.

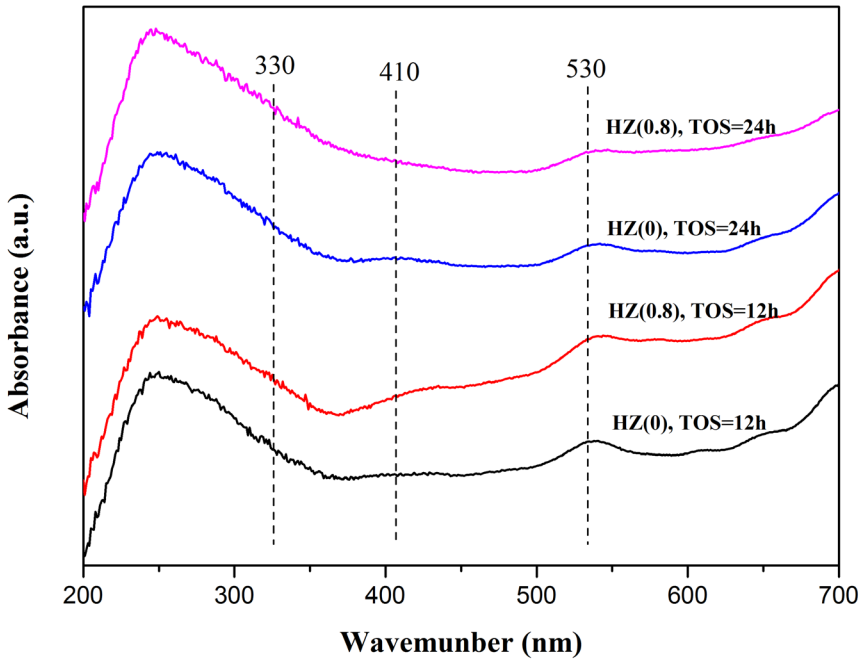

Figure 9. DR UV-vis spectra of the catalysts obtained in different TOS.

In order to acquire more information of reaction species deposited in the used catalysts at different TOS, FTIR spectroscopy was carried out. Figure 10 depicts the FTIR spectra of the used HZ(0) and HZ(0.8) catalyst after reactions at different TOS (12 and 24 h), denoted as HZ(0)-12, HZ(0)-24, HZ(0.8)-12 and HZ(0.8)-24, respectively.

According to previous researches [24,32–35], the bands at 1300–1500 cm^{-1} are not assigned, as a variety of bands overlapped in this region; the band at approximately 1506, 1520, 1540, 1558 cm^{-1} are assigned to monoenyl carbenium ions, non-condensed aromatics, alkylnaphthalenes and/or

polyphylenes; the band at ~1600 cm^{-1} is attributed to polyaromatics and/or condensed coke; another two bands at 1625 and 1635 cm^{-1} are due to double bonds or olefins. As shown in Figure 10A, the band at 1625 cm^{-1} are increased slightly for HZ(0.8)-12 sample compared to sample HZ(0)-12; the band at 1600 and 1625 cm^{-1} are rasied remarkable for HZ(0.8)-24 compared with HZ(0)-24, indicating that HZ(0.8) catalyst has more polyaromatics or double bonds coke species than HZ(0) catalyst at the same TOS. For HZ(0.8) catalysts at different TOS, polyaromatics and double bonds coke species are increased with increasing reaction time. As mentioned above, these two catalysts have similar textual properties and exhibit similar morphology, so coke contents were not affected by diffusion of products. This phenomenon is contributed to the higher fraction of Al_F pairs in the catalyst, which enhances the oligomerization of alkenes and cyclization reactions to promote the formation of aromatics.

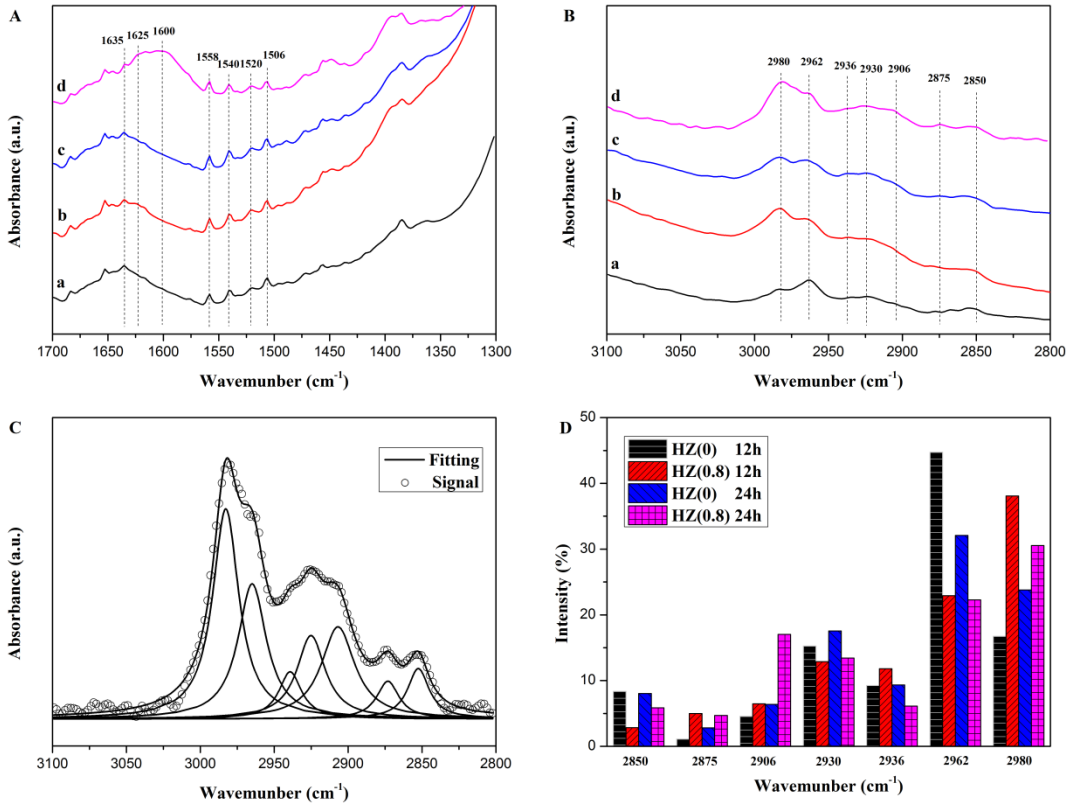

Figure 10. FTIR spectra of the used HZ(0) and HZ(0.8) catalysts after propane aromatization for 12 and 24 h at 550 °C with WHSV of propane being 0.6 h^{-1} and N_2/C_3H_8 ratio being 2.5 in feedstock in the region of (**A**) 1700–1300 cm^{-1} and (**B**) 3100–2800 cm^{-1} for (a) HZ(0)-12, (b) HZ(0.8)-12, (c) HZ(0)-24, (d) HZ(0.8)-24; (**C**) Deconvoluted CH-region (3100–2800 cm^{-1}) spectrum of HZ(0.8)-24; (**D**) Fraction of intensity (calculated using the area of the peaks in (**B**) of several characteristic vibrational bands of the catalysts in the FTIR region 2800–3100 cm^{-1}.

The bands between 2800 and 3100 cm^{-1} are assigned to aliphatic and aromatic C–H vibrations. As shown in Figure 10B, the bands in 3000–3100 cm^{-1} ascribed to aromatic C–H vibration are not observed in the used catalysts, probably because most of the deposited coke species are fused-ring aromatics and/or highly branched cokes, which exhibit low C–H intensity [33,34].

In order to quantify the coke vibrations, the spectrum of each sample is deconvoluted into several Lorentzian peaks [32,35]: 2850 cm^{-1}, $–CH_2$ groups related to symmetric paraffinic hydrocarbons; 2875 cm^{-1}, $–CH_3$ groups related to symmetric paraffinic hydrocarbons; 2906~2937 cm^{-1}, –CH and $–CH_2$ groups of asymmetric paraffinic hydrocarbons; 2962 cm^{-1}, $–CH_3$ groups of asymmetric paraffinic hydrocarbons; 2980 cm^{-1}, –CH and $–CH_2$ groups related to symmetric olefinic hydrocarbons with high carbon number. An example of the deconvolution is depicted in Figure

10C where the region of 2800–3100 cm^{-1} is plotted for the HZ(0.8)-24 sample. As shown in Figure 10D, the band intensities at 2962 cm^{-1} of used HZ(0) catalyst are much higher than that of used HZ(0.8) catalyst at the same TOS, while the band intensity at 2980 cm^{-1} show the opposite, indicating that HZ(0.8) catalyst possesses less paraffinic hydrocarbons species and more olefinic hydrocarbons species with high carbon number. With the increase of TOS, the band intensity at 2980 cm^{-1} is increased for the used HZ(0.8) catalysts, but it is decreased for the used HZ(0) catalysts. As mentioned above, this band at 2980 cm^{-1} is assigned to –CH and $–CH_2$ groups related to symmetric olefinic hydrocarbons with high carbon number, which is oligomerized from the oligomerization of lower olefins in the propane aromatization. This result suggested that the oligomer olefins are decreased on HZ(0.8) catalyst with the time on stream. Combined with the result obtained from Figures 10A(b,d), it is convinced that the higher olefins have been further converted into aromatics on HZ(0.8) catalyst with the time on stream.

This FTIR analysis of coke species on the used catalysts demonstrates that higher Al_F pairs content in the catalyst promotes the oligomerization and cyclization reactions of olefins and leads to the production of more aromatics, which is in good agreement with the results of the catalytic performance tests and Operando DR UV-vis spectra experiments.

2.5. DFT Calculations

DFT calculations were used to further evaluate the influence of the structure of single Al_F and Al_F pairs on the propane aromatization process. Here, 1-hexyl cation was applied as reactant to form benzene, because 1-hexyl cation is a typical precursor species (formed by propene [36]) in propane aromatization. The aromatization of 1-hexyl cation undergoes cyclization, hydride transfer, and dehydrogenation to produce aromatics. As shown in Scheme 2, 1-hexyl cation firstly produces the cyclohexane through cyclization reaction (TS1). Then, the hydride transfer reaction (TS2) between cyclohexane and propoxy leads to the formation of cyclohexyl carbenium ion and propane. After that, the cyclohexyl carbenium ion is converted to benzene by repeated deprotonations and hydride transfer reactions (TS3 and TS4). The calculated kinetic and thermodynamic results are given in Table 6. It should be noticed the deprotonation reaction are not considered because the free energy barrier of deprotonation reaction is quite low, in comparison with that of cyclization and hydride transfer reactions [37].

It was found that the ZSM-5 zeolite containing Al_F pairs shows lower free energy barrier and higher rate constants of cyclization (171 kJ mol^{-1}, 2.50 × 10^2 s^{-1}) and hydride transfer (145–159 kJ mol^{-1}, 1.38 × 10^3–1.03 × 10^4 s^{-1}) reactions than the ZSM-5 zeolite containing single Al (176 kJ mol^{-1} and 1.12 × 10^2 s^{-1} for cyclization, and 156–166 kJ mol^{-1} and 5.11 × 10^2–2.06 × 10^3 s^{-1} for hydride transfer). Meanwhile, the low free energy barriers for cyclization and hydride transfer steps on ZSM-5 zeolite containing Al_F pairs, is mainly contributed to their lower enthalpy barriers. These results demonstrate that the structure of Al_F pairs in the framework of HZSM-5 zeolite shows stronger electrostatic stabilization effect on the transition states than that of single Al_F [38,39]. Therefore, it can better promote the aromatization process and produce more aromatic species.

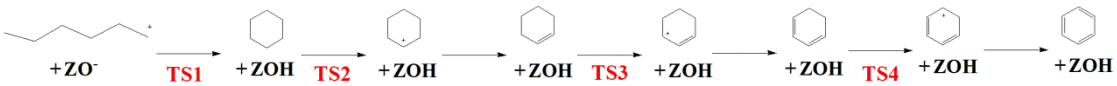

Scheme 2. Reaction network for the formation of benzene in the transition period for propane aromatization over H-ZSM-5 catalysts. ZOH and ZO^- represent the protonated and deprotonated acid sites of zeolite, respectively.

Table 6. Calculated free energy barriers ($\Delta G_{int}^{\neq}$), rate constants (k), enthalpy barriers ($\Delta H_{int}^{\neq}$), and entropy losses ($-T\Delta S_{int}^{\neq}$), as well as reaction free energies (ΔG_R) at 823 K for each reaction step in the formation of benzene in the transition period for propane aromatization over H-ZSM-5.

Step	$\Delta G_{int}^{\neq}$ (kJ mol^{-1})	k (s^{-1})	$\Delta H_{int}^{\neq}$ (kJ mol^{-1})	$-T\Delta S_{int}^{\neq}$ (kJ mol^{-1})	ΔG_R (kJ mol^{-1})
			Single Al_F		
TS1	176	1.12×10^2	157	19	−19
TS2	158	1.75×10^3	160	−2	105
TS3	156	2.06×10^3	151	5	9
TS4	166	5.11×10^2	158	8	−1
			Al_F pairs		
TS1	171	2.50×10^2	151	20	−28
TS2	145	1.03×10^4	154	−9	108
TS3	149	5.34×10^3	143	6	27
TS4	159	1.38×10^3	149	10	10

3. Experimental Section

3.1. Catalyst Preparation

The ZSM-5 zeolites with different contents of Al_F pairs were synthesized by adjusting the Na/Al molar ratios (0, 0.4, 0.8 and 1.1) in the precursor gels. The Na-free gel contained tetraethyl orthosilicate (TEOS), tetrapropylammonium hydroxide (TPAOH, 25 wt.%) and aluminum nitrate ($Al(NO_3)_3$) in a composition proportion of 1 SiO_2 : 0.0125 Al_2O_3 : 0.4 TPAOH : 66 H_2O. The chemical composition of Na^+-containing gels was 1 SiO_2 : 0.0125 Al_2O_3 : 0.4 TPAOH: x NaCl : 36 H_2O, where x was 0.01, 0.02 and 0.0275, corresponding to the samples with Na/Al ratios of 0.4, 0.8 and 1.1, respectively. The gel was stirred at room temperature for 12 h before being sealed into a Teflon-lined autoclave. After crystallation at 170 °C for 5 d, the material was centrifugated, washed with water, dried overnight at 100 °C, and calcined at 560 °C for 10 h in air to obtain the parent NaZSM-5 zeolite.

H-form ZSM-5 was prepared by repeated ion exchanging NaZSM-5 zeolite with NH_4NO_3 aqueous solution (1 M, m(liquid)/m(solid) = 40) at 80 °C for 4 h, which was then calcined at 550 °C for 6 h in air. The samples were donated as HZ(m), where m is the Na/Al molar ratio in the precusor gel. The normal Si/Al molar ratio of all samples was 40.

To investigate the Al distribution in the framework of ZSM-5 zeolites, Co-ZSM-5 samples were prepared by reverse ion exchanging of HZSM-5 with NaCl aqueous solution (1.0 M) at 80 °C for 6 h and subsequent ion exchanging of NaZSM-5 three times with a $Co(NO_3)_2$ aqueous solution (0.05 M) at 80 °C for 12 h under stirring condition. The Co-ZSM-5 sample was rinsed with distilled water three times, dried in air and calcined at 500 °C for 4 h in air [17].

3.2. Catalyst Characterization

X-ray powder diffraction (XRD) patterns were collected on a MiniFlex II desktop X-ray diffractometer (Rigaku, Japan) with Cu $K\alpha$ radiation (0.154 nm, 30 kV, 15 mA). The cell parameters of the catalysts were obtained by Rietveld refinement of XRD data using X'Pert HighScore Plus software (PANalytical, Holland).

The scanning electron microscopy (SEM) images were taken on a field emission scanning electron microscope (FESEM, JSM 7001-F, JEOL, Japan).

Nitrogen adsorption/desorption measurements were performed at 77 K on a TriStar II 3020 gas adsorption analyzer (Micromeritics, Norcross, GA, USA). Prior to the measurement, the zeolite sample was degassed at 300 °C for 8 h. The total specific surface area was calculated by Brunauer-Emmett-Teller (BET) method; the total pore volume was estimated from the volume of nitrogen adsorbed at a nitrogen relative pressure of 0.99. The pore size distribution was acquired by the Density Functional Theory (DFT) method. The micropore volume and external surface area were measured by t-plot method. The micropore surface area was obtained from the difference between the total pore surface area and the external surface area.

The chemical composition of the catalysts was determined by Inductively Coupled Plasma Optical Emission Spectrometer (ICP-OES, Thermo iCAP6300, Thermo Fisher Scientific, Waltham, MA, USA).

The ultraviolet-visible diffuse reflectance spectra (UV-vis-DRS) were measured on an Cary 5000 UV-vis-NIR spectrophotometer (Agilent, Wilmington, DE, USA) equipped with a poly (tetrafluoroethylene) integrating sphere. The UV-vis DRS of Co^{2+}-exchanged samples were collected at room temperature after dehydration at 773 K for 5 h under high vacuum condition (<10^{-1} Pa). The concentration of Al_{single} and Al_{pairs} was calculated using the following equations:

$$[Al_{single}] = [Al_{total}] - 2[Co_{max}] \quad (1)$$

$$[Al_{pairs}] = 2[Co_{max}] \quad (2)$$

where $[Al_{total}]$ and $[Co_{max}]$ are the Al content and Co content in Co-type ZSM-5 zeolites, respectively, and both were determined by ICP-OES.

FTIR spectra were measured on a Tensor 27 spectrometer (Bruker, Germany) in the range 400–4000 cm^{-1} with a resolution of 4 cm^{-1} by the conventional KBr method at room temperature and 10^{-2} Pa.

Pyridine-adsorption infrared (Py-IR) spectra were measured on a Bruker Tensor 27 FTIR spectrometer. Before collecting the spectrum, the self-supported sample wafer was evacuated at 350 °C and 10^{-2} Pa for 2 h, and cooled to room temperature subsequently. Then pyridine vapor was introduced into the sample cell for 1 h. The spectrum was collected after evacuation of the sample wafer at 150 °C for 1 h. The contents of Brønsted and Lewis acid sites were estimated using the following equation by integrating the vibration bands at 1540 and 1450 cm^{-1}, respectively:

$$C = \frac{A}{\varepsilon} \times \frac{S}{M} \times 1000 \quad (3)$$

where C is the concentration of Brønsted and Lewis acid sites (μmol g^{-1}), A is the area of the vibration band at 1540 or 1450 cm^{-1}, S is the surface area of the sample wafer (1.33 cm^2), ε is the molar extinction coefficient (1.13 and 1.28 cm μmol^{-1} for Brønsted and Lewis acid sites, respectively), and M is the mass of sample (mg) [26].

Temperature-programmed desorption of NH_3 (NH_3-TPD) was performed on an AutoChem II 2920 chemisorption analyzer from Micromeritics (USA). A catalyst sample (0.1 g) was first pretreated at 550 °C for 2 h in Ar stream (30 mL/min) and then cooled to 120 °C. Then gaseous NH_3 (5 vol % in argon, 30 mL/min) was introduced into the sample tube for 30 min to saturated adsorb of NH_3 on the catalyst. After that, the physically adsorbed NH_3 was removed by Ar (30 mL/min) at 120 °C for 2 h. To get the NH_3-TPD profile, the catalyst was then heated from 120 to 500 °C at a ramp of 10 °C/min; the desorption signal was recorded by a thermal conductivity detector (TCD).

Thermal gravimetric analysis (TGA) of the used catalysts were performed on a Rigaku Thermo plus Evo TG 8120 (Tokyo, Japan) instrument at a heating rate of 10 °C/min in an air flow (30mL/min). The coke content deposited on the catalysts was determined by weight loss between 400 and 700 °C.

^{27}Al MAS NMR spectra were measured on Bruker Avance III 600 MHz Wide Bore spectrometer (Bruker, Germany) operating at a magnetic field of 14.2 T. The spectra were acquired at a spinning rate of 13 kHz with a π/12 pulse width of 1.0 μs and a recycle delay of 1 s.

Operando diffuse reflectance ultraviolet-visible (DR UV-vis) spectra were obtained using an Agilent Cary 5000 UV-vis-NIR spectrophotometer (Agilent, Wilmington, DE, USA). The self-supporting sample wafer (100 mg) was placed in a self-made quartz cell. The samples were pretreated at 250 °C under a flow of Ar (30 mL/min) at atmospheric pressure for 2 h. The spectra were obtained at 250 °C under a flow of propene (1 mL/min) at atmospheric pressure.

3.3. Catalysis tests

3.3.1. Propane Conversion in a Fixed-Bed Reactor

The catalytic test for propane aromatization was carried out on a fixed-bed reactor (i.d. 10 mm) at atmospheric pressure. Fixed-bed reaction process was illustrated in Figure 11. Typically, 2.3 g of catalyst (20–40 mesh) was used per round. The reaction was carried out at 550 °C in a propane/nitrogen flow (42 mL/min) with a N_2/C_3H_8 molar ratio of 2.5 viz. a weight hourly space velocity (WHSV) of propane being 0.6 h^{-1}. The gas and liquid products were separated with a cold trap. The gaseous products including H_2, CH_4, light olefins and paraffins were analyzed on-line on a gas chromatograph (GC) (Agilent 7890A) equipped with a thermal conductivity detector (TCD, MoleSieve 5A column, 3 m × 1/16 inch × 1 μm) and two flame ionization detectors (FIDs, GC-OxyPlot column, 10 m × 530 μm × 10 μm; Al_2O_3 column, 50 m × 530 μm × 15 μm). The liquid products including C_{5+} non-aromatics and aromatics were analyzed by another Agilent 7890A gas chromatograph equipped with a FID and a capillary column (Agilent 19091S-001, 50 m × 200 μm × 0.5 μm). The propane conversion and product selectivity were calculated as below:

$$X_{Propane} = \frac{\sum C_i - C_{propane}}{\sum C_i} \times 100\% \quad (4)$$

$$S_i = \frac{C_i}{\sum C_i - C_{propane}} \times 100\% \quad (5)$$

where $X_{propane}$ (%) is the conversion of propane, S_i (wt.%) is the selectivity to the target product i; C_i and $C_{propane}$ (wt.%) are the corrected mass concentration for species i and propane, respectively.

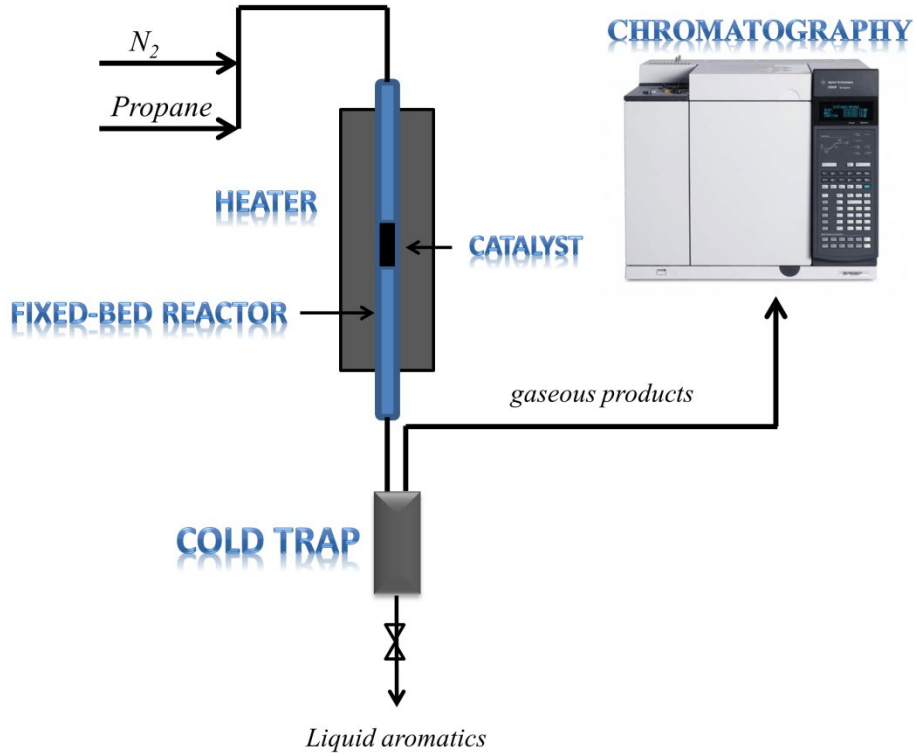

Figure 11. Schematic diagram of fixed-bed reaction process.

3.3.2. Propane Conversion in a Micro Reactor

In order to estimate the initial products, conversion of propane was performed in a U-shaped quartz tube micro reactor with an inner diameter of 6 mm. About 100 mg of catalyst (20–40 mesh)

was loaded in the reactor bed. The reaction was carried out at 500 °C in a propane/nitrogen flow (42 mL/min) as described above. The whole products at a time-on-stream of 2 min were analyzed on-line on a GC as mentioned above. Relative concentration of each product was obtained by dividing the calibrated chromatographic areas of the product by methane concentration since methane results mainly from protolytic cracking of propane on the zeolite protonic sites [3,40].

3.3.3. Pulse Reaction Test of Propane Conversion

Pulse reaction test of propane conversion was also conducted in the U-shaped quartz tube reactor as mentioned above. The catalyst was pretreated in a N_2 flow (20 mL/min) at 500 °C for 3 h. Then 2.0 mL propane was injected into the U-shaped quartz tube along with a N_2 flow (20 mL/min). After 10 s, the carrier gas (N_2) was switched out. The quartz tube was quenched in liquid nitrogen immediately after 70 s later of the injection. The retained products in the catalyst were dissolved in 20 wt.% HF aqueous solution and subsequently extracted with CH_2Cl_2. The extracts, with hexachloroethane as an internal standard (I.S.), were analyzed on a Shimadzu GCMS-QP2010 gas chromatography-mass spectrometry (GC-MS) system equipped with an Rtx-5MS capillary column (60 m × 0.25 mm × 0.25 μm).

3.4. DFT Calculation

The catalytic kinetic and thermodynamic parameters (details see Table 6) of each reaction step in aromatization process were calculated on the basis of two 120 T cluster models containing the single Al and Al pairs. As shown in Figure 12, for the model of single Al, one Al atom substituted one Si atom at T12 site, whereas two Al atoms substituted two Si atoms at T12 and T7 sites to form the sequence of Al-O-(Si-O)$_2$-Al in one ring of zeolite framework. The peripheral silicon atoms were saturated with hydrogen atoms; the distance between hydrogen and silicon atoms (Si–H bond) was 1.47 Å, and the direction of which was the same as that of Si–O bond. Density functional theory (DFT) calculations of the catalytic kinetics were performed with the Gaussian 09.D01 package [41]. Details can be found in our former work [26].

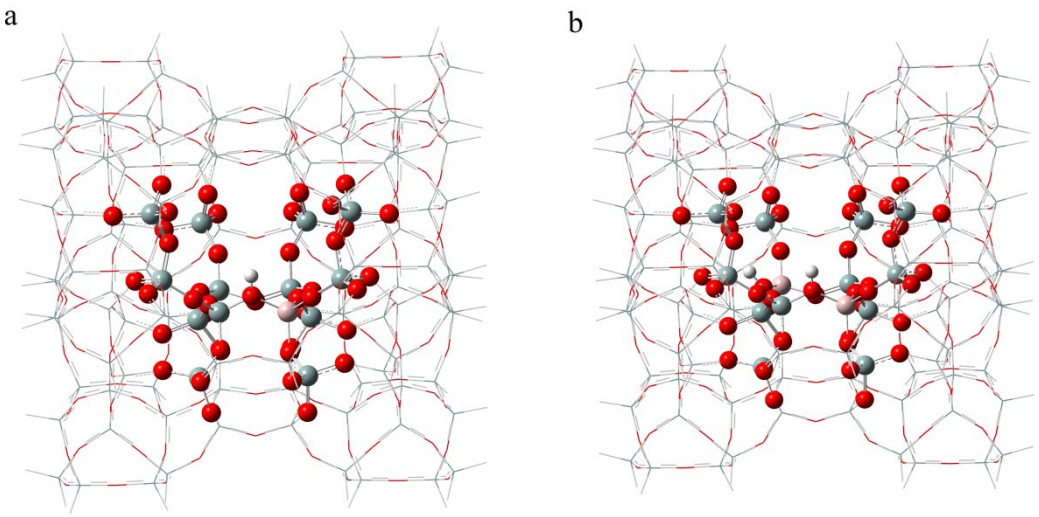

Figure 12. The model of single Al (**a**) and Al pairs (**b**) of 120T cluster model over H-ZSM-5. Atom coloring: gray (Si), red (O), white (H), and pink (Al).

4. Conclusions

Series ZSM-5 catalysts containing different Al_F pair contents (54.2% to 64.4%) were synthesized by controlling the Na/Al molar ratios (0–1.1) in the precursor gels. The obtained ZSM-5 catalysts with similar Si/Al_F mole ratio, textual properties, morphology, but different Al_F pairs concentration were applied to propane aromatization reactions. A linear correlation has been established between

the propane conversion/selectivity of aromatics and Al_F pairs content. The catalyst HZ(0.8) (Na/Al molar ratio 0.8 in the gel) with the highest paired Al_F concentration shows the highest propane conversion (38.2%) and aromatics selectivity (19.7 wt.%), which is about 1.5 times (for conversion) and almost 2.5 times (for aromatics selectivity) higher than that of HZ(0) catalyst. Propane pulse experiment, micro reactor activity estimation, Operando diffuse reflectance ultraviolet-visible (DR UV-vis) spectra and FTIR characterization of coke species on the used catalysts suggest that the present of more Al_F pairs in the ZSM-5 framework promotes the oligomerization and cyclization reactions of olefins and leads to the production of more aromatics. DFT calculation results indicate that the HZSM-5 zeolite containing Al_F pairs shows lower free energy barrier and higher rate constants for cyclization and hydride transfer reactions than the HZSM-5 zeolite containing single Al_F; the structure of Al_F pairs in the HZSM-5 zeolite exhibits stronger electrostatic stabilization effect on the transition states than that of single Al_F. This study provided a theoretical guidance to design catalysts for propane aromatization.

Author Contributions: H.W., H.Z. and W.F. conceived and designed the experiments; D.S. carried out most of the experiments and characterizations; S.W. performed all the DFT calculations; D.S. and S.W. co-wrote the manuscript; P.W., L.Z., Z.Q. and J.W. discussed the results and gave many valuable suggestions for improving the work. All authors have read and agreed to the published version of the manuscript.

Funding: This work was financially supported by the National Natural Science Foundation of China (21773281, 21991092, U1910203, 21802157, U1862101 and 21875275), Natural Science Foundation of Shanxi Province of China (201901D211581 and 201801D221092).

Acknowledgments: The calculations are performed on the Computer Network Information Center of Chinese Academy of Sciences.

Conflicts of Interest: The authors declare no conflict of interest.

References

1. Bhan, A.; Delgass, W.N. Propane Aromatization over HZSM-5 and Ga/HZSM-5 Catalysts. *Catal. Rev.* **2008**, *50*, 19–151.
2. Zhang, P.; Tan, L.; Yang, G.; Tsubaki, N. One-pass selective conversion of syngas to paraxylene. *Chem. Sci.* **2017**, *8*, 7941–7946.
3. Guisnet, M.; Gnep, N.S.; Alario. F. Aromatization of short chain alkanes on zeolite catalysts. *Appl. Catal. A-Gen.* **1992**, *89*, 1–30.
4. Al-Yassir, N.; Akhtar, M.N.; Al-Khattaf, S. Physicochemical properties and catalytic performance of galloaluminosilicate in aromatization of lower alkanes: A comparative study with Ga/HZSM-5. *J. Porous Mater.* **2012**, *19*, 943–960.
5. Su, X.; Wang, G.; Bai, X.; Wu, W.; Xiao, L.; Fang, Y.; Zhang, J. synthesis of nanosized HZSM-5 zeolites isomorphously substituted by gallium and their catalytic performance in the aromatization. *Chem. Eng. J.* **2016**, *293*, 365–375.
6. Choudhary, V.R.; Sivadinarayana, C.; Kinage, A.K.; Devadas, P.; Guisnet, M. H-Gallosilicate (MFI) propane aromatization catalyst Influence of calcination temperature on acidity, activity and deactivation due to coking. *Appl. Catal. A-Gen.* **1996**, *136*, 125–142.
7. Montes, A.; Giannetto, G. A new way to obtain acid or bifunctional catalysts: V. Considerations on bifunctionality of the propane aromatization reaction over [Ga,Al]-ZSM-5 catalysts. *Appl. Catal. A-Gen.* **2000**, *197*, 31–39.
8. Rodrigues, V.O.; Faro Júnior, A.C. On catalyst activation and reaction mechanisms in propane aromatization on Ga/HZSM5 catalysts. *Appl. Catal. A-Gen.* **2012**, *435*, 68–77.
9. Choudhary, V.R.; Kinage, A.K.; Sivadinarayana, C.; Devadas, P.; Sansare, S.D.; Guisnet, M. H-Gallosilicate (MFI) Propane Aromatization Catalyst: Influence of Si/Ga Ratio on Acidity, Activity and Deactivation Due to Coking. *J. Catal.* **1996**, *158*, 34–50.
10. Han, J.; Jiang, G.; Han, S.; Liu, J.; Zhang, Y.; Liu, Y.; Wang, R.; Zhao, Z.; Xu, C.; Wang, Y.; et al. The Fabrication of Ga_2O_3/ZSM-5 Hollow Fibers for Efficient Catalytic Conversion of n-Butane into Light Olefins and Aromatics. *Catalysts* **2016**, *6*, 13–25.

11. Al-Yassir, N.; Akhtar, M.N.; Ogunronbi, K.; Al-Khattaf, S. Synthesis of stable H-galloaluminosilicate MFI with hierarchical pore architecture by surfactant-mediated base hydrolysis, and their application in propane aromatization. *J. Mol. Catal. A-Chem.* **2012**, *360*, 1–15.
12. Guisnet, M.; Gnep, N.S.; Aittaleb, D.; Doyemet, Y.J. Conversion of light alkanes into aromatic hydrocarbons: VI. Aromatization of C2-C4 alkanes on H-ZSM-5—Reaction mechanisms. *Appl. Catal. A-Gen.* **1992**, *87*, 255–270.
13. Biscardi, J.A.; Iglesia, E.; Isotopic Tracer Studies of Propane Reactions on H− ZSM5 Zeolite. *J. Phys. Chem. B* **1998**, *102*, 9284–9289.
14. Meriaudeau, P.; Naccache, C. Further Evidence on the Change of Acid Properties of H-ZSM-5 by Ga and Pt. *J. Catal.* **1995**, *157*, 283–288.
15. Biscardi, J.A.; Meitzner, G.D.; Iglesia, E. Structure and Density of Active Zn Species in Zn/H-ZSM5 Propane Aromatization Catalysts. *J. Catal.* **1998**, *179*, 192–202.
16. Dedecek, J.; Kaucky, D.; Wichterlova, B.; Gonsiorova, O. Co^{2+} ions as probes of Al distribution in the framework of zeolites. ZSM-5 study. *Phys. Chem. Chem. Phys.* **2002**, *4*, 5406–5413.
17. Liang, T.; Chen, J.; Qin, Z.; Li, J.; Wang, P.; Wang, S.; Wang, G.; Dong, M.; Fan, W.; Wang, J. Conversion of Methanol to Olefins over H-ZSM-5 Zeolite: Reaction Pathway Is Related to the Framework Aluminum Siting. *ACS Catal.* **2016**, *6*, 7311−7325.
18. Wang, S.; Wang, P.; Qin, Z.; Chen, Y.; Dong, M.; Li, J.; Zhang, K.; Liu, P.; Wang, J.; Fan, W. Relation of Catalytic Performance to the Aluminum Siting of Acidic Zeolites in the Conversion of Methanol to Olefins, Viewed via a Comparison between ZSM-5 and ZSM-11. *ACS Catal.* **2018**, *8*, 5485–5505.
19. Biligetu, T.; Wang, Y.; Nishitob, T.; Otomo, R.; Park, S.; Mochizuki, H.; Kondo, J.N.; Tatsumi, T.; Yokoi, T. Al distribution and catalytic performance of ZSM-5 zeolites synthesized with various alcohols. *J. Catal.* **2017**, *353*, 1–10.
20. Sazama, P.; Dedecek, J.; Gábová, V.; Wichterlová, B.; Spoto, G.; Bordiga, S. Effect of aluminium distribution in the framework of ZSM-5 on hydrocarbon transformation. Cracking of 1-butene. *J. Catal.* **2008**, *254*,180–189.
21. Yokoi, T.; Mochizuki, H.; Namba, S.; Kondo, J.N.; Tatsumi, T. Control of the Al distribution in the framework of ZSM-5 zeolite and its evaluation by solid-state NMR technique and catalytic properties. *J. Phys. Chem. C* **2015**, *119*, 15303–15315.
22. Bjorgen, M.; Svelle, S.; Joensen, F.; Nerlov, J.; Kolboe, S.; Bonino, F.; Palumbo, L.; Bordiga, S.; Olsbye, U. Conversion of methanol to hydrocarbons over zeolite H-ZSM-5: On the origin of the olefinic species. *J. Catal.* **2007**, *249*,195–207.
23. Song, C.; Chu, Y.; Wang, M.; Shi, H.; Zhao, L.; Guo, X.; Yang, W.; Shen, J.; Xue, N.; Peng, L.; et al. Cooperativity of adjacent Brønsted acid sites in MFI zeolite channel leads to enhanced polarization and cracking of alkanes. *J. Catal.* **2017**, *349*,163–174.
24. Tabor, E.; Bernauer, M.; Wichterlová, B.; Dedecek, J. Enhancement of propene oligomerization and aromatization by proximate protons in zeolites; FTIR study of the reaction pathway in ZSM-5. Catal. *Sci. Technol.* **2019**, *9*, 4262–4275.
25. Li, J.; Ma, H.; Chen, Y.; Xu, Z.; Li, C.; Ying, W. Conversion of methanol to propylene over hierarchical HZSM-5: The effect of Al spatial distribution. *Chem. Commun.* **2018**, *54*, 6032–6035.
26. Wang, S.; Li, S.; Zhang, L.; Qin, Z.; Dong, M.; Li, J.; Wang, J.; Fan, W. Insight into the effect of incorporation of boron into ZSM-11 on its catalytic performance for conversion of methanol to olefins. *Catal. Sci. Technol.* **2017**, *7*, 4766–4779.
27. Dai, W.; Wu, G.; Li, L.; Guan, N.; Hunger, M. Mechanisms of the Deactivation of SAPO-34 Materials with Different Crystal Sizes Applied as MTO Catalysts. *ACS Catal.* **2013**, *3*, 588–596.
28. Bjørgen, M.; Bonino, F.; Kolboe, S.; Lillerud, K.-P.; Zecchina, A.; Bordiga, S. Spectroscopic Evidence for a Persistent Benzenium Cation in Zeolite H-Beta. *J. Am. Chem. Soc.* **2003**, *125*, 15863–15868.
29. Wulfers, M.J.; Jentoft, F.C. Identification of carbonaceous deposits formed on H-mordenite during alkane isomerization. *J. Catal.* **2013**, *307*, 204–213.
30. Borodina, E.; Sharbini Harun Kamaluddin, H.; Meirer, F.; Mokhtar, M.; Asiri, A.M.; Al Thabaiti, S.A.; Basahel, S.N.; Ruiz-Martinez, J.; Weckhuysen, B.M. Influence of the Reaction Temperature on the Nature of the Active and Deactivating Species During Methanol-to-Olefins Conversion over H-SAPO-34. *ACS Catal.* **2017**, *7*, 5268–5281.

31. Borodina, E.; Meirer, F.; Lezcano-Gonzalez, I.; Mokhtar, M.; Asiri, A.M.; Al-Thabaiti, S.A.; Basahel, S.N.; Ruiz-Martinez, J.; Weckhuysen, B.M. Influence of the Reaction Temperature on the Nature of the Active and Deactivating Species during Methanol to Olefins Conversion over H-SSZ-13. *ACS Catal.* **2015**, *5*, 992–1003.
32. Xue, Y.; Li, J.; Wang, S.; Cui, X.; Dong, M.; Wang, G.; Qin, Z.; Wang, J.; Fan, W. Co-reaction of methanol with butene over a high-silica H-ZSM-5 catalyst. *J. Catal.* **2018**, *367*, 315–325.
33. Song, C.; Liu, K.; Zhang, D.; Liu, S.; Li, X.; Xie, S.; Xu, L. Effect of cofeeding n-butane with methanol on aromatization performance and coke formation over a Zn loaded ZSM-5/ZSM-11 zeolite. *Appl. Catal. A-Gen.* **2014**, *470*, 15–23.
34. Hernandez, E.D.; Jentoft, F.C. Spectroscopic Signatures Reveal Cyclopentenyl Cation Contributions in Methanol-to-Olefins Catalysis. *ACS Catal.* **2020**, *10*, 5764–5782.
35. Emdadi, L.; Mahoney, L.; Lee, I.C.; Leff, A.C.; Wu, W.; Liu, D.; Nguyen, C.K.; Tran, D.T. Assessment of coke deposits on lamellar metal-modifed MFI zeolites in ethylene transformation to aromatic liquids. *Appl. Catal. A-Gen.* **2020**, *595*, 117510–117520.
36. Maksoud, W.A.; Gevers, L.E.; Vittenet, J.; Ould-Chikh, S.; Telalovic, S.; Bhatte, K.; Abou-Hamad, E.; Anjum, D.H.; Hedhili, M.N.; Vishwanath, V.; et al. A strategy to convert propane to aromatics (BTX) using TiNp 4 grafted at the periphery of ZSM-5 by surface organometallic chemistry. *Dalton Trans.* **2019**, *48*, 6611–6620.
37. Wang, C.; Wang, Y.; Du, Y.; Yang, G.; Xie, Z. Similarities and differences between aromatic-based and olefin-based cycles in H-SAPO-34 and H-SSZ-13 for methanol-to-olefins conversion: Insights from energetic span model. *Catal. Sci. Technol.* **2015**, *5*, 4354–4364.
38. Wang, S.; Chen, Y.; Wei, Z.; Qin, Z.; Ma, H.; Dong, M.; Li, J.; Fan, W.; Wang, J. Polymethylbenzene or alkene cycle? theoretical study on their contribution to the process of methanol to olefins over H-ZSM-5 zeolite. *J. Phys. Chem. C* **2015**, *119*, 28482–28498.
39. Wang, S.; Chen, Y.; Qin, Z.; Zhao, T.; Fan, S.; Dong, M.; Li, J.; Fan, W.; Wang, J. Origin and evolution of the initial hydrocarbon pool intermediates in the transition period for the conversion of methanol to olefins over H-ZSM-5 zeolite. *J. Catal.* **2019**, *369*, 382–395.
40. Guisnet, M.; Gnep, N.S. Aromatization of propane over GaHMFI catalysts. Reaction scheme, nature of the dehydrogenating species and mode of coke formation. *Catal. Today* **1996**, *31*, 275–292.
41. Frisch, M.J.; Trucks, G.W.; Schlegel, H.B.; Scuseria, G.E.; Robb, M.A.; Cheeseman, J.R.; Scalmani, G.; Barone, V.; Mennucci, B.; Petersson, G.A.; et al. *Gaussian 09, Revision D.01*; Gaussian, Inc.: Wallingford, CT, USA, 2009.